Voltage-induced modulation of interfacial ionic liquids measured using surface plasmon resonant grating nanostructures *⊙*

Special Collection: Festschrift in honor of Louis E. Brus

Indu Aravind ^⑤; Yu Wang ^⑥; Zhi Cai ^⑥; Ruoxi Li ^⑥; Rifat Shahriar ^⑥; George N. Gibson ^⑥; Ernest Guignon; Nathaniel C. Cady ^⑥; William D. Page ^⑥; Arturo Pilar; Stephen B. Cronin [™] ^⑥



J. Chem. Phys. 161, 034702 (2024)

https://doi.org/10.1063/5.0202642





What are your needs for periodic signal detection?



Find out more





Voltage-induced modulation of interfacial ionic liquids measured using surface plasmon resonant grating nanostructures

Cite as: J. Chem. Phys. 161, 034702 (2024); doi: 10.1063/5.0202642 Submitted: 6 February 2024 • Accepted: 26 June 2024 •







Published Online: 15 July 2024



Indu Aravind, DYu Wang, DZhi Cai, DRuoxi Li, DRuoxi Li, DRifat Shahriar, DGeorge N. Gibson, Sibson, Si







AFFILIATIONS

- Department of Physics and Astronomy, University of Southern California, Los Angeles, California 90089, USA
- ²Mork Family Department of Chemical Engineering and Materials Science, University of Southern California, Los Angeles, California 90089, USA
- Ming Hsieh Department of Electrical Engineering, University of Southern California, Los Angeles, California 90089, USA
- Department of Physics, University of Connecticut, Storrs, Connecticut 06269, USA
- ⁵Ciencia Inc., East Hartford, Connecticut 06108, USA
- ⁶Colleges of Nanoscale Science and Engineering, SUNY Polytechnic Institute, Albany, New York 12203, USA
- Department of Chemistry, University of Southern California, Los Angeles, California 90089, USA

Note: This paper is part of the JCP Festschrift in Honor of Louis E. Brus.

a) Author to whom correspondence should be addressed: scronin@usc.edu

ABSTRACT

We have used surface plasmon resonant metal gratings to induce and probe the dielectric response (i.e., electro-optic modulation) of ionic liquids (ILs) at electrode interfaces. Here, the cross-plane electric field at the electrode surface modulates the refractive index of the IL due to the Pockels effect. This is observed as a shift in the resonant angle of the grating (i.e., $\Delta \phi$), which can be related to the change in the local index of refraction of the electrolyte (i.e., Δn_{local}). The reflection modulation of the IL is compared against a polar (D₂O) and a non-polar solvent (benzene) to confirm the electro-optic origin of resonance shift. The electrostatic accumulation of ions from the IL induces local index changes to the gratings over the extent of electrical double layer (EDL) thickness. Finite difference time domain simulations are used to relate the observed shifts in the plasmon resonance and change in reflection to the change in the local index of refraction of the electrolyte and the thickness of the EDL. Simultaneously using the wavelength and intensity shift of the resonance enables us to determine both the effective thickness and Δn of the double layer. We believe that this technique can be used more broadly, allowing the dynamics associated with the potential-induced ordering and rearrangement of ionic species in electrode-solution interfaces.

Published under an exclusive license by AIP Publishing. https://doi.org/10.1063/5.0202642

INTRODUCTION

Recently, there has been considerable speculation surrounding the behavior of room temperature ionic liquids at charged electrochemical (i.e., electrode) interfaces; 1-7 however, the structure and spatial profile of such interfacial charge remain largely elusive. The behavior of electrolytes at electrode interfaces is of great interest for a variety of chemical and biological processes ranging from electrocatalysis to bio-membranes. Many research groups are studying these interfaces using various techniques, including atomic force

microscopy, 1,2 sum frequency generation (SFG) spectroscopy, 8,9 and anisotropic fluorescence depth profiling measurements. Wang et al. reported a large Pockels effect in room temperature ionic liquids with a charge-induced change in the index of refraction of $\Delta n = 0.3.6$ However, the mechanism underlying these strong electrooptic effects is still a topic of some debate and may arise from a charge-induced long-range ordering of the ionic liquid that extends over length scales of 100 μ m, as observed by the anisotropic fluorescence depth profiling measurements of Ma et al.7 Krishna et al. reported charge profiling using three-dimensional (3D) atomic force microscopy (CP-3D-AFM) to experimentally quantify the real-space charge distribution of the electrode surface and electrical double layers (EDLs) with angstrom depth resolution and found that these charged interfacial layers extend over ~1 nm.1,2 In, yet, another study, Toda et al. reported the observation of the Pockels effect in ionic liquids through voltage-induced changes in the Raman spectra. 10,111 From this, they concluded that the length scale of the ordering in the ILs is 10-100 nm, extending more than would be expected for the electrical double layer but not as far as the micrometer scale reported by Ma et al.7 As such, this five order of magnitude discrepancy (i.e., 100 µm vs 1 nm) has created somewhat of a controversy within the field. Several theory groups have explored the interfacial structure of metal/ionic liquid (IL) systems using ab initio molecular dynamics simulations; however, a large gap currently exists between these simulations and experimental measurements, and improved techniques for exploring the structure of these interfacial layers are much needed. 12-19 The importance of further exploring the electric field effects on ILs to unravel the intricacies of interfacial structures and their control is pivotal for advancing their functionalities.

Surface plasmon resonant gratings have been used to detect small changes in the index of refraction for many years. 20-23 This phenomenon has largely been used for detecting the presence of biomolecules and biomarkers through surface functionalization, enabling applications in non-invasive cancer diagnosis and drug discovery. 24 Several research groups have explored the Pockels effect using low-angle optical measurements. 10,25,26 The SPR approach is advantageous because it selectively probes a small volume, within just a few nanometers of the electrode surface, without being

influenced by the dielectric constant of the bulk solution. SPR sensors have been previously used to study the time relaxation associated with the IL interfacial layers. ^{27,28} However, combining the experimental observations with electromagnetic simulations to explore the structure of the electrical double layer and Pockels effect at electrochemical/electrode interfaces in ionic liquids is still underexplored. Here, we use the sensitivity of surface plasmon sensors to interfacial index changes to explore voltage-induced changes, explore potential ordering at interfaces, and compare ILs, water, and dielectric solvents. This method enables us to investigate the dynamics linked to the ordering and rearrangement of the double layer.

RESULTS AND DISCUSSION

In our work, we have used metallic grating structures that support surface plasmon resonance in the visible light spectrum to monitor changes in the refractive index at the interface between the ionic liquid (IL) and the electrode, due to the application of an electric potential. The complex propagation constant of surface plasmons is sensitive to the refractive index profile of the surrounding medium. When an electric field is applied across the IL, it alters the refractive index profile, impacting the conditions required for surface plasmon excitation. By observing alterations under the resonant excitation conditions (such as wavelength, angle, and polarization) of the optical wave interacting with the surface plasmon, we can infer changes in the medium's refractive index. We measure the strength of coupling between monochromatic light and the grating structure across various angles of incidence and observe the change

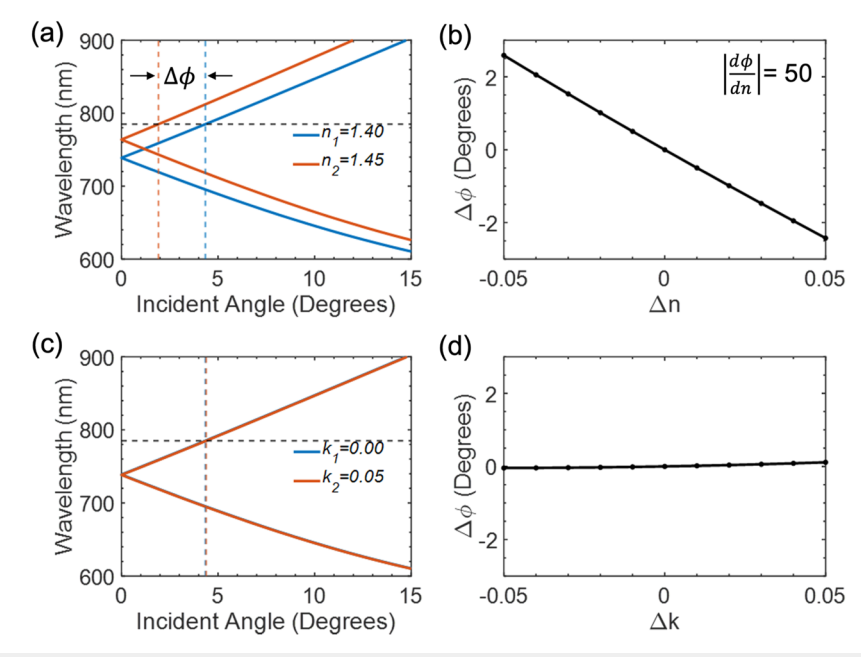


FIG. 1. (a) First-order plasmon resonant mode and (b) shift in plasmon resonant angle at 785 nm plotted as a function of the index of refraction of the surrounding media for a 500 nm corrugated Au grating (k = 0). (c) Change in band diagram and (d) shift in plasmon resonant angle at 785 nm as a function of the imaginary part of the surrounding media index for a 500 nm corrugated Au grating (n = 1.4).

in the incidence angle, yielding the strongest coupling with the surrounding index profile perturbation. To excite the surface plasmons in the grating structure, the momentum and energy of the incident photons must match those of the surface plasmons (i.e., wave vector matching). The incident angles that satisfy this condition at each wavelength can be found by solving the following equation:^{29–31}

$$\frac{2\pi n_d}{\lambda} \sin \phi + m \frac{2\pi}{a} = \pm \left(\text{Re} \left\{ \frac{\omega}{c} \left(\frac{\varepsilon_d \varepsilon_m}{\varepsilon_d + \varepsilon_m} \right)^{\frac{1}{2}} \right\} \right), \tag{1}$$

where a is the periodicity of the grating, m is the order of the surface plasmon mode, ϕ is the incidence angle, and ε_m and ε_d are the dielectric functions of the metal and the surrounding medium, respectively.31 Figure 1 shows the first-order surface plasmon mode in our corrugated gold grating with a 500 nm period obtained analytically using Eq. (1). Figure 1(a) shows the shift in resonance when the real part of the refractive index of the surrounding medium changes by 0.05 RIU (Refractive Index Unit) from a nominal medium index of n = 1.4 and k = 0. The resonant shift depends on the wavelength of the surface plasmon excitation and the local slope of the band diagram at the wavelength. Figure 1(b) shows the resonance angle at a wavelength of 785 nm plotted as a function of the change in the real part of the refractive index of the surrounding medium ($\Delta n_{\text{effective}}$). The slope of this curve represents the sensitivity of our measurement technique with this grating design and is estimated to be $S = \frac{d\phi}{dn} = 50^{\circ}/\text{RIU}$. The change in the imaginary part of the medium index (k) has a minimal effect on the resonance shift, as evident from Figs. 1(c) and 1(d). For a Δk of 0.1, the resonant angle shift is negligible.

EXPERIMENTAL SECTION

For our electro-optic measurements, we employed a microfluidic cell comprising an ionic liquid encapsulated between a gold (Au) grating and a gold-coated calcium fluoride (CaF₂) window with an optically transparent aperture in the center. In Fig. 2(a), the schematic outlines the design of the sample cell, where a ~1 mm thick polydimethylsiloxane (PDMS) stamp with a rectangular opening secures the ionic liquid sandwiched between the Au grating and the CaF2 window. We have used the ionic liquid [DEME⁺][TFSI⁻] (diethylmethyl(2-methoxyethyl)ammonium bis(trifluoromethylsulfonyl)imide) for this experiment. An electric potential is applied across the IL using electrodes attached to the grating and the gold-coated CaF2 window. Figure 2(b) shows the cross-sectional SEM image of the 500 nm pitch Au grating structure used in this experiment. These gratings are fabricated by depositing 100 nm Au on a corrugated Si structure, patterned by photolithography and reactive ion etching (RIE), as reported previously. We sweep through the plasmon resonance by varying the incident angle of monochromatic light at a wavelength of 785 nm. Figure 2(c) shows the schematic that demonstrates our setup for reflection measurements, where the polarization of the incoming light is oriented perpendicular to the grating lines (p-polarization) by means of a half-wave plate. The sample cell is attached to a motorized rotational stage, and the reflection from the grating is measured at different incident angles using a silicon photodetector (Thorlabs S121C). We observe sharp dips in the photoreflectance around ±4.6°, corresponding to the conditions under which there

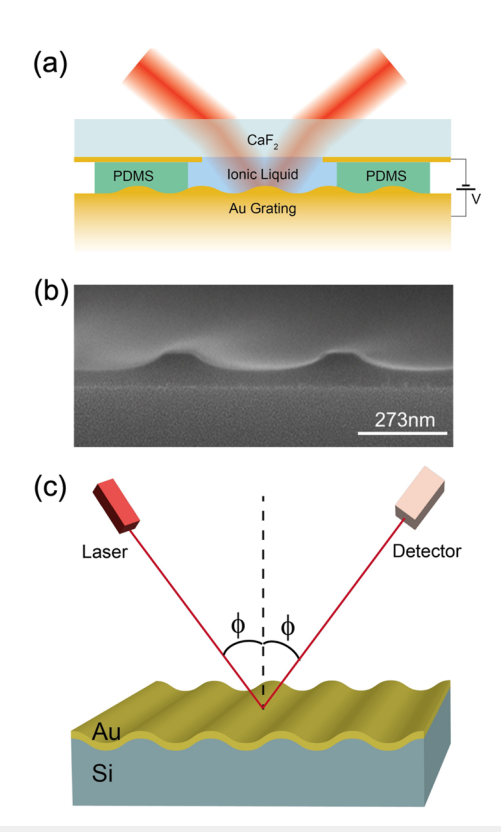


FIG. 2. (a) Schematic diagram of the electrochemical cell used for the electro-optic measurement. (b) Cross-sectional SEM image of the 500 nm pitch corrugated Au grating structure. (c) Schematic diagram of the angle-dependent photo-reflection measurement setup.

is wave vector matching between the incident light and the spacing in the grating. 0,33-36 Figure 3 illustrates the variation in reflected power as the incident angle is swept from -10° to 10° under applied voltages of 0 and 3 V. A notable shift in the plasmon resonance toward smaller angles by $\Delta \phi = 0.35^{\circ}$ is observed upon application of the electric potential. In addition to the angle shift, the peak reflectivity reduces with the applied potential as well. Under an applied potential of 3 V, a reflection change of 18% is observed [(18.27 - 14.94 mW)/18.27 mW = 18.2%]. This resonance shift, which vanishes upon removal of the applied potential, is consistently repeatable across several experiments, as evidenced in Fig. 3. When a uniform perturbation of the refractive index permeates the entire ionic liquid (IL) medium, resulting in a bulk refractive index change, this shift in the resonant angle equates to an effective refractive index alteration in the IL of $\Delta n_{\rm effective} = 0.35/S = 0.007$, where S denotes the sensitivity determined in Fig. 1(b). The effective index change agrees well with the electro-optic index changes in ILs previously reported in the literature.1

Changes in the refractive index of ionic liquids under an applied electric field can mainly be attributed to the development of an electrical double layer (EDL) at the interface, resulting from the electro-migration of cationic and anionic species. Previous studies have shown that cations and anions are alternately stacked to form

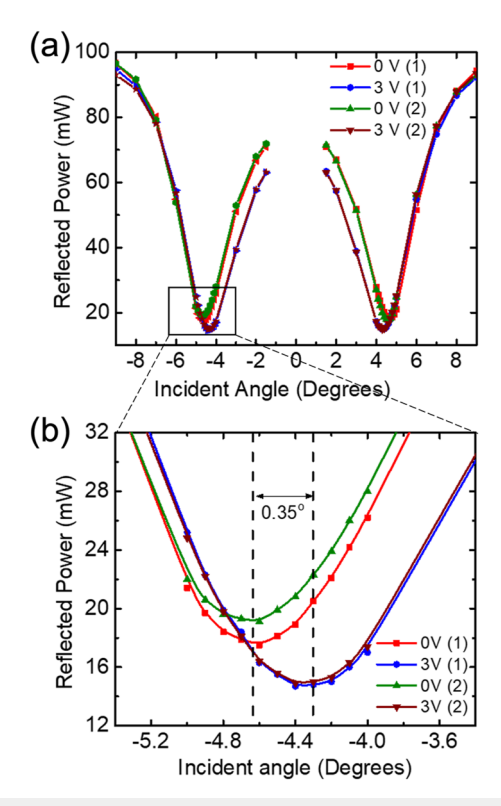


FIG. 3. (a) Angle-dependent reflection for different voltages applied across the ionic liquid electrolyte. (b) Zoomed-in plot of the reflection profile in the range (a) -5.4° and -3.2° .

an interfacial layer, with its structure influenced by the sign of the surface potential, as well as the disparities in size, shape, and surface interactions among the ionic species.³⁷ Toda et al. found that applying a potential to ionic liquids (ILs) caused uniform intensity changes in Raman spectra, independent of cation and anion vibrational modes. They attributed this to the Pockels effect, where the potential induces the ordering of ILs near the electrode interface.¹ Wang et al. also reported the surface charge-induced birefringence in ionic liquids (ILs) due to alterations in the electrical double layer (EDL) with the applied potential.⁶ The molecular ordering induced in the ionic liquid near the electrode interface breaks the inversion symmetry, enabling the manifestation of the Pockels effect within the interfacial domain, which subsequently alters the refractive index as detected in experimental measurements. Conventional narratives, which imply a uniform change in medium index, fail to acknowledge the crucial aspect of electric field-induced molecular ordering near the electrode interface. It has been postulated that a conformal interfacial layer, extending a finite distance (h) from the electrode surface, facilitates the analysis of the well-defined electrode-ionic liquid interface through the application of the ray optics model.¹¹ Although these models do not fully encapsulate the role of an intermediate layer, which acts as a transitional zone between the highly organized interfacial layer and the bulk liquid, they provide a framework for delineating the structural transformations occurring during molecular assembly.

NUMERICAL MODEL

In our system, we have modeled the EDL as a thin conformal layer above the corrugated grating with a characteristic thickness of h and a dielectric constant of $\varepsilon_d + \delta \varepsilon_d$ (or index of $n + \Delta n_{local}$). The perturbation in the surface index change affects the surface plasmon wave vector and thereby the conditions of excitation required to excite the resonance. For thicknesses much larger than the penetration depth of the surface plasmon, the change in surface plasmon wave vector converges to the same as in the case of bulk refractive index change.³⁸ By employing computational electromagnetic tools to simulate the Pockels effect in ionic liquids using a thin conformal layer characterized by variable refractive indices and layer thicknesses, a more profound understanding of the interfacial layer's characteristics can be achieved. This approach enables a comparative analysis between theoretical predictions and experimental findings, thereby yielding enhanced insights into the interfacial layer's dynamics.

A commercial Finite Difference Time Domain (FDTD) solver (Ansys Lumerical FDTD solutions) is used to solve Maxwell's equations discretely in time and space for the grating structure. The geometry of the corrugated grating surface is fitted to a measured AFM (Atomic Force Microscope) cross-sectional profile using the following equation:

$$y(x) = A \left[\frac{1}{1 + e^{\alpha(x - w)/a}} + \frac{1}{1 + e^{-\alpha(x + w)/a}} \right],$$
 (2)

where a is the periodicity of the grating (a = 500 nm), A is the height difference between the peaks and valleys of the corrugation (corrugation amplitude), α specifies the slope of the corrugation, and w determines the length of the flat top of the grating. By fitting the surface geometry with Eq. (2), the fit parameters are obtained as A = 54 nm, w = 0.25a, and α = 25. Using the momentum matching condition [Eq. (1)] and Snell's law, the refractive index of the bulk IL is estimated be equal to 1.41 to satisfy the resonant angle (ϕ _o = 4.6°) at 785 nm illumination.

We have simulated the reflection from the grating structure as a function of angle of incidence in the presence of an EDL. A 785 nm plane wave source is used to illuminate the grating structure at an oblique angle. The reflection from the grating is monitored using a power monitor placed behind the source as a function of the angle of incidence. Figure 4(a) shows the simulated angular reflection of the grating as a function of the EDL thickness (h) for a fixed index change (Δn_{local}) of the interfacial EDL, and Fig. 5(b) shows the same as a function of the EDL index perturbation for a fixed thickness of the EDL. The reflection from the grating as a function of angle reaches a minimum value when the maximum coupling condition is satisfied (corresponds to the resonant excitation condition). For positive index perturbation, the resonance shifts to lower angles with an increase in both Δn_{local} and h. The change in index also affects the resonant reflection from the structure. The reflection initially goes down with an increase in Δn_{local} and then goes up. The change in reflection is mainly from the change in the index of EDL and is in alignment with the expectation from Fresnel's equations. The sensitivity of the resonance shift to both the thickness and index of EDL can be explained by the near-field perturbation. Figure 5 shows the resonant field profile simulated using FDTD with and without an interfacial EDL. When the medium is a homogenous layer of the IL

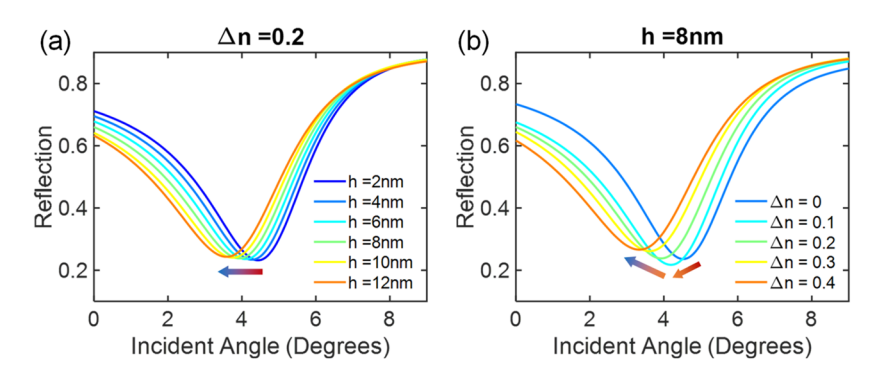


FIG. 4. Resonance shift with (a) the thickness of EDL for a constant local index change and (b) the perturbed index of EDL with a constant thickness.

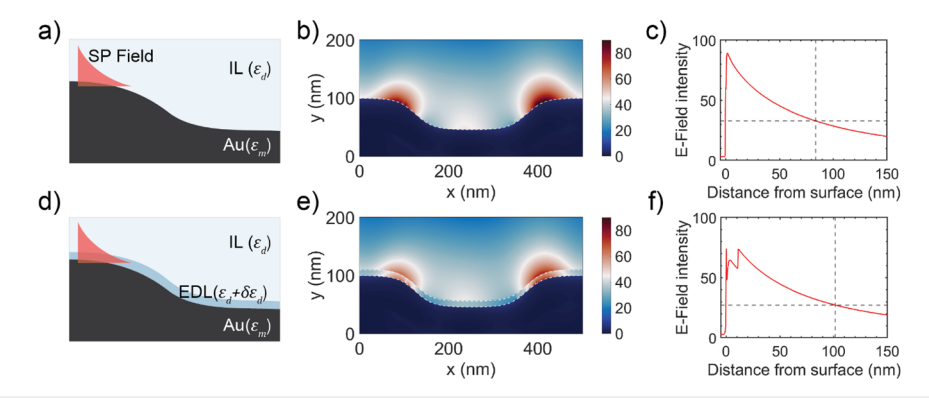


FIG. 5. (a) Interface of Au grating and homogeneous ionic liquid medium. (b) Electric field intensity distribution and (c) field decay away from the metal for grating with homogeneous ionic liquid medium. (d) Interface of Au grating and ionic liquid medium with a conformal EDL. (e) Electric field intensity distribution and (f) field decay away from the metal for grating with the EDL interface.

as shown in Fig. 6(a), the plasmonic field decays exponentially away from the Au surface. The field is concentrated at the peak to trough transition region of the grating. The penetration depth (L_{pd}) of the surface plasmon excitation into the ionic liquid medium is estimated to be 84 nm, as shown in Fig. 5(c). The resonant field profile with an interfacial EDL of 10 nm thickness and 0.1 RIU index change is plotted in Fig. 5(e). The cross-sectional field profile in Fig. 5(f) clearly shows the perturbation of a smoothly decaying field due to the introduction of EDL. If the thickness of the EDL is smaller than the surface plasmon penetration depth, it can perturb the surface plasmon field and, consequently, affect the plasmon wave vector. The sensitivity of the surface plasmons to the EDL thickness goes down with an increase in thickness. Beyond the penetration depth, the plasmonic system cannot distinguish the EDL from a bulk index change.

The h and perturbed refractive Δn of the interfacial layer are varied, and the corresponding change in resonant excitation is simulated using FDTD. Figures 6(a) and 6(b) illustrate the simulated shifts in resonant angle ($\Delta \phi$) and variations in resonant reflectivity ($\Delta R/R$), respectively, contingent upon h and $\Delta n_{\rm local}$. The white contour in Fig. 6(a) represents the required refractive index change and corresponding thickness necessary to induce a resonance shift of $\Delta \phi = -0.35^{\circ}$, as observed in measurements. This contour line estab-

lishes an empirical correlation between the thickness and refractive index adjustment of the interfacial layer, enabling the estimation of the EDL's thickness based on the refractive index change of the conformal layer, and vice versa. In the bulk phase, the ionic liquid exhibits a random assortment of ionic species. However, applying an electrical bias close to the interface encourages greater organization of ions, thereby amplifying the refractive index alteration of the conformal layer. Remarkably, to achieve a given resonant angle shift, the requisite thickness (h) increases exponentially with minor perturbations in the index.

When the EDL forms near the grating with a local index perturbation, the reflectivity of the structure changes compared to the bulk medium. The reflection change is highly sensitive to the local index change, but relatively independent of the EDL thickness. The reflectivity changes remain almost constant as h increases. The simulations have revealed that the reflection from the structure decreases for small local index changes (small Δn_{local}) and increases for sufficiently large local index changes (large Δn_{local}). The maximum reflectivity drop observed in the simulation with a conformal index perturbation is around 11%, which is lower than what is observed in the measurements. This discrepancy could be due to the abrupt boundary and uniform layer thickness assumption of the double layer in the simulation. From Figs. 6(a) and 6(b), we obtain an

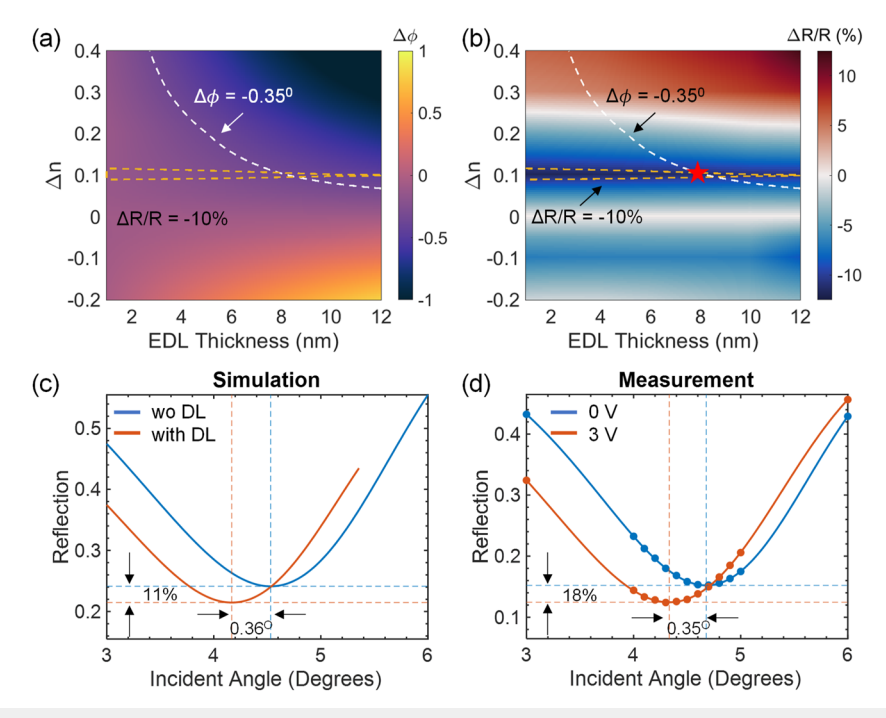


FIG. 6. (a) Simulated electric field profile calculated on resonance. (b) Plasmonic electric field intensity as it decays away from the metal surface. (c) Plasmon resonance shift as a function of the change in refractive index and thickness of the ionic liquid double layer. The contour tracks the combination of index change and thickness required to satisfy the experimentally observed shift of -0.35° with the applied potential. (b) Change in reflection from the grating as the double layer forms as a function of the change in refractive index and thickness of the ionic liquid double layer. The contours represent the combination of index change and thickness required to obtain a resonance shift of $\Delta \phi = -0.35^{\circ}$ and 10% decrease in reflection. The red star represents the intersection point. (c) Simulated and (d) measured reflection as a function of incident angle to the grating with and without an ionic liquid double layer.

h that produces a resonant angle shift of $\Delta \phi = -0.35^{\circ}$ and a reflectivity change of $\Delta R/R = 11\%$, respectively. The h of 8 nm indicated by the red star in Fig. 6(b) represents the approximate thickness derived from the simulations that correspond to the changes in refractive index from the experiment. Figure 6(c) shows the shifts in the simulated reflection spectra of the SPR grating structure using an EDL thickness of 8 nm and a local change in refractive index of Δn_{local} = 0.1 with respect to the bulk IL medium without any EDL. The measured response with and without an applied potential is shown in Fig. 6(d) and qualitatively agrees with the simulations. The plasmonic sensor offers the opportunity to probe into the dynamics of the EDL formation. It was also observed that the ionic liquid exhibits a strong asymmetric response with the polarity of the applied bias. It can be inferred that the index shift in the interfacial layer is asymmetric with the polarity of the immediate layer. In addition, it was observed that the time constant of the optical response is much higher than that of the current response.2

In conclusion, we have used surface plasmon resonant Au gratings to measure the refractive index change due to the Pockels effect created at the interface of polar liquid and metal gratings under an applied electrochemical voltage. We observe a voltage-induced change of $\Delta\phi=0.35^\circ$ in the plasmon resonant angle at an excitation wavelength of 785 nm, which corresponds to an effective index change of $\Delta n_{\rm effective}=0.007$, which is of the same order reported in previous studies. ^{11,26} The electrostatic accumulation of ions from

ILs induces local index changes to the gratings over the extent of the electrical double layer (EDL). Finite difference time domain (FDTD) simulations are used to relate the observed shifts in the plasmon resonance and change in reflection to the change in the local index of refraction of the electrolyte. The angular and intensity changes of the resonance enable us to determine the change in index Δn_{local} of the double layer. We believe that this technique can be used more broadly, allowing the dynamics associated with the potential-induced ordering and rearrangement of ionic species at electrode–solution interfaces to be measured, provided that the EDL is within the surface plasmon penetration depth.

SUPPLEMENTARY MATERIAL

The supplementary material provides the details of the materials used, additional data of temporal dynamics of positive and negative biases, resonant shift of the IL with the polarity of the electrode potential, sensing depth vs sensitivity trade-off, and electro-optic modulation of water.

ACKNOWLEDGMENTS

This research was supported by the Army Research Office (ARO) Award No. W911NF-22-1-0284 (I.A.); the U.S. Depart-

ment of Energy, Office of Basic Energy Sciences, Award No. DE-SC0019322 (R.L.); National Science Foundation (NSF), Award Nos. CHE-2106480 (S.W.) and CBET-2012845 (Y.W.); and Air Force Office of Scientific Research (AFOSR), Grant No. FA9550-19-1-0115 (B.Z.). The fabrication and characterization were carried out in Ciencia, Inc. and USC Core Center of Excellence in Nano Imaging (CNI).

AUTHOR DECLARATIONS

Conflict of Interest

The authors have no conflicts to disclose.

Author Contributions

Indu Aravind: Conceptualization (equal); Data curation (equal); Formal analysis (equal); Investigation (equal); Methodology (equal); Writing - original draft (equal). Yu Wang: Conceptualization (supporting); Data curation (supporting); Methodology (supporting); Supervision (supporting). Zhi Cai: Data curation (supporting); Investigation (supporting); Methodology (supporting); Resources (supporting). Ruoxi Li: Data curation (supporting); Investigation (supporting); Resources (supporting). Rifat Shahriar: Data curation (equal). George N. Gibson: Resources (supporting). Ernest Guignon: Resources (supporting). Nathaniel C. Cady: Resources (supporting). William D. Page: Resources (supporting). Arturo Pilar: Resources (supporting). Stephen B. Cronin: Conceptualization (equal); Funding acquisition (equal); Methodology (equal); Project administration (equal); Resources (equal); Supervision (equal); Writing - original draft (equal); Writing - review & editing (equal).

DATA AVAILABILITY

The data that support the findings of this study are available from the corresponding author upon reasonable request.

REFERENCES

- ¹ K. S. Panse, H. Wu, S. Zhou, F. Zhao, N. R. Aluru, and Y. Zhang, "Innermost ion association configuration is a key structural descriptor of ionic liquids at electrified interfaces," J. Phys. Chem. Lett. 13, 9464–9472 (2022).
- ²L. K. S. Bonagiri, K. S. Panse, S. Zhou, H. Wu, N. R. Aluru, and Y. Zhang, "Real-space charge density profiling of electrode–electrolyte interfaces with angstrom depth resolution," ACS Nano 16, 19594–19604 (2022).
- ³Y. Wang, G. M. Swain, and G. J. Blanchard, "Charge-induced birefringence in a room-temperature ionic liquid," J. Phys. Chem. B 125, 950–955 (2021).
- ⁴Y. Wang, F. Parvis, M. I. Hossain, K. Ma, R. Jarošová, G. M. Swain, and G. J. Blanchard, "Local and long-range organization in room temperature ionic liquids," Langmuir 37, 605–615 (2021).
- ⁵K. Ma, R. Jarosova, G. M. Swain, and G. J. Blanchard, "Modulation of an induced charge density gradient in the room-temperature ionic liquid BMIM⁺BF₄-," J. Phys. Chem. C **122**, 7361–7367 (2018).
- ⁶Y. Wang, L. Adhikari, G. A. Baker, and G. J. Blanchard, "Cation structure-dependence of the Pockels effect in aprotic ionic liquids," Phys. Chem. Chem. Phys. **24**, 18067–18072 (2022).
- ⁷K. Ma, R. Jarosova, G. M. Swain, and G. J. Blanchard, "Charge-induced longrange order in a room-temperature ionic liquid," Langmuir 32, 9507–9512 (2016).

- ⁸ A. Montenegro, A. E. Vaughn, M. Mammetkuliyev, B. Zhao, B. Zhang, H. Shi, D. Bhattacharyya, A. V. Benderskii, and S. B. Cronin, "Field-dependent orientation and free energy of D₂O at an electrode surface observed via SFG spectroscopy," J. Phys. Chem. C **126**, 20831–20839 (2022).
- ⁹A. Montenegro, C. Dutta, M. Mammetkuliev, H. Shi, B. Hou, D. Bhattacharyya, B. Zhao, S. B. Cronin, and A. V. Benderskii, "Asymmetric response of interfacial water to applied electric fields," Nature **594**, 62–65 (2021).
- ¹⁰H. Kanemaru, S. Yukita, H. Namiki, Y. Nosaka, T. Kobayashi, and E. Tokunaga, "Giant Pockels effect of polar organic solvents and water in the electric double layer on a transparent electrode," RSC Adv. 7, 45682–45690 (2017).
- ¹¹S. Toda, R. Clark, T. Welton, and S. Shigeto, "Observation of the Pockels effect in ionic liquids and insights into the length scale of potential-induced ordering," Langmuir 37, 5193–5201 (2021).
- ¹² B. V. Merinov, S. V. Zybin, S. Naserifar, S. Morozov, J. Oppenheim, W. A. Goddard III, J. Lee, J. H. Lee, H. E. Han, Y. C. Choi, and S. H. Kim, "Interface structure in Li-metal/[Pyr₁₄] [TFSI]-ionic liquid system from ab initio molecular dynamics simulations," J. Phys. Chem. Lett. 10, 4577–4586 (2019).
- ¹³ M. Y. Yang, B. V. Merinov, S. V. Zybin, W. A. Goddard Iii, E. K. Mok, H. J. Hah, H. E. Han, Y. C. Choi, and S. H. Kim, "Transport properties of imidazolium based ionic liquid electrolytes from molecular dynamics simulations," Electrochem. Sci. Adv. 2, e2100007 (2022).
- ¹⁴G. Feng, S. Li, V. Presser, and P. T. Cummings, "Molecular insights into carbon supercapacitors based on room-temperature ionic liquids," J. Phys. Chem. Lett. 4, 3367–3376 (2013).
- ¹⁵E. Heid, S. Boresch, and C. Schröder, "Polarizable molecular dynamics simulations of ionic liquids: Influence of temperature control," J. Chem. Phys. 152, 094105 (2020).
- ¹⁶H. Zhang, M. Zhu, W. Zhao, S. Li, and G. Feng, "Molecular dynamics study of room temperature ionic liquids with water at mica surface," Green Energy Environ. 3, 120–128 (2018).
- ¹⁷P. Ray, A. Balducci, and B. Kirchner, "Molecular dynamics simulations of lithium-doped ionic-liquid electrolytes," J. Phys. Chem. B 122, 10535–10547 (2018).
- ¹⁸Z. Yan, D. Meng, X. Wu, X. Zhang, W. Liu, and K. He, "Two-dimensional ordering of ionic liquids confined by layered silicate plates via molecular dynamics simulation," J. Phys. Chem. C **119**, 19244–19252 (2015).
- ¹⁹F. Federici Canova, M. Mizukami, T. Imamura, K. Kurihara, and A. L. Shluger, "Structural stability and polarisation of ionic liquid films on silica surfaces," Phys. Chem. Chem. Phys. 17, 17661–17669 (2015).
- ²⁰ J. Homola, I. Koudela, and S. S. Yee, "Surface plasmon resonance sensors based on diffraction gratings and prism couplers: Sensitivity comparison," Sens. Actuators, B 54, 16–24 (1999).
- ²¹ P. S. Vukusic, G. P. Bryan-Brown, and J. R. Sambles, "Surface plasmon resonance on gratings as a novel means for gas sensing," Sens. Actuators, B **8**, 155–160 (1992).
- ²²S. Long, J. Cao, Y. Wang, S. Gao, N. Xu, J. Gao, and W. Wan, "Grating coupled SPR sensors using off the shelf compact discs and sensitivity dependence on grating period," Sens. Actuators Rep. 2, 100016 (2020).
- grating period," Sens. Actuators Rep. 2, 100016 (2020).

 ²³ J. S. Yuk, E. F. Guignon, and M. A. Lynes, "Sensitivity enhancement of a grating-based surface plasmon-coupled emission (SPCE) biosensor chip using gold thickness," Chem. Phys. Lett. 591, 5–9 (2014).
- ²⁴S. Roh, T. Chung, and B. Lee, "Overview of the characteristics of microand nano-structured surface plasmon resonance sensors," Sensors 11, 1565–1588 (2011).
- ²⁵D. Hayama, K. Seto, K. Yamashita, S. Yukita, T. Kobayashi, and E. Tokunaga, "Giant Pockels effect in an electrode-water interface for a 'liquid' light modulator," OSA Continuum 2, 3358–3373 (2019).
- ²⁶ A. Okada, T. Kobayashi, and E. Tokunaga, "Interfacial Pockels effect of solvents with a larger static dielectric constant than water and an ionic liquid on the surface of a transparent oxide electrode," Appl. Sci. 12, 2454 (2022).
- ²⁷S. Zhang, N. Nishi, and T. Sakka, "Electrochemical surface plasmon resonance measurements of camel-shaped static capacitance and slow dynamics of electric double layer structure at the ionic liquid/electrode interface," J. Chem. Phys. 153, 044707 (2020).
- ²⁸N. Nishi, Y. Hirano, T. Motokawa, and T. Kakiuchi, "Ultraslow relaxation of the structure at the ionic liquid|gold electrode interface to a potential step probed

- by electrochemical surface plasmon resonance measurements: Asymmetry of the relaxation time to the potential-step direction," Phys. Chem. Chem. Phys. 15, 11615–11619 (2013).
- ²⁹Y. Wang, I. Aravind, Z. Cai, L. Shen, G. N. Gibson, J. Chen, B. Wang, H. Shi, B. Song, E. Guignon, N. C. Cady, W. D. Page, A. Pilar, and S. B. Cronin, "Hot electron driven photocatalysis on plasmon-resonant grating nanostructures," ACS Appl. Mater. Interfaces 12, 17459–17465 (2020).
- ³⁰I. Aravind, Y. Wang, Z. Cai, L. Shen, B. Zhao, S. Yang, Y. Wang, J. M. Dawlaty, G. N. Gibson, E. Guignon, N. C. Cady, W. D. Page, A. Pilar, and S. B. Cronin, "Hot electron plasmon-resonant grating structures for enhanced photochemistry: A theoretical study," Crystals 11, 118 (2021).
- J. Homola, "Electromagnetic theory of surface plasmons," in *Surface Plasmon Resonance Based Sensors*, edited by J. Homola (Springer, Berlin, Heidelberg, 2006), pp. 3–44.
 L. Shen, G. N. Gibson, N. Poudel, B. Hou, J. Chen, H. Shi, E. Guignon,
- ³²L. Shen, G. N. Gibson, N. Poudel, B. Hou, J. Chen, H. Shi, E. Guignon, N. C. Cady, W. D. Page, A. Pilar, and S. B. Cronin, "Plasmon resonant amplification of hot electron-driven photocatalysis," Appl. Phys. Lett. **113**, 113104 (2018).
- ³³L. Shen, N. Poudel, G. N. Gibson, B. Hou, J. Chen, H. Shi, E. Guignon, W. D. Page, A. Pilar, and S. B. Cronin, "Plasmon resonant amplification of a hot electron-driven photodiode," Nano Res. 11, 2310–2314 (2018).

- ³⁴Y. Wang, L. Shen, Y. Wang, B. Hou, G. N. Gibson, N. Poudel, J. Chen, H. Shi, E. Guignon, N. C. Cady, W. D. Page, A. Pilar, J. Dawlaty, and S. B. Cronin, "Hot electron-driven photocatalysis and transient absorption spectroscopy in plasmon resonant grating structures," Faraday Discuss. 214, 325–339 (2019).
 ³⁵Y. Wang, H. Shi, L. Shen, Y. Wang, S. B. Cronin, and J. M. Dawlaty,
- ³⁵Y. Wang, H. Shi, L. Shen, Y. Wang, S. B. Cronin, and J. M. Dawlaty, "Ultrafast dynamics of hot electrons in nanostructures: Distinguishing the influence on interband and plasmon resonances," ACS Photonics **6**, 2295–2302 (2019).
- ³⁶Y. Wang, Y. Wang, I. Aravind, Z. Cai, L. Shen, B. Zhang, B. Wang, J. Chen, B. Zhao, H. Shi, J. M. Dawlaty, and S. B. Cronin, "In situ investigation of ultrafast dynamics of hot electron-driven photocatalysis in plasmon-resonant grating structures," J. Am. Chem. Soc. 144, 3517–3526 (2022).
- ³⁷T. Douglas, S. Yoo, and P. Dutta, "Ionic liquid solutions show anomalous crowding behavior at an electrode surface," Langmuir 38, 6322–6329 (2022).
- ³⁸ J. Homola and M. Piliarik, "Surface plasmon resonance (SPR) sensors," in *Surface Plasmon Resonance Based Sensors*, edited by J. Homola (Springer, Berlin, Heidelberg, 2006), pp. 45–67.
- ³⁹X. Luo, S. Deng, and P. Wang, "Temporal–spatial-resolved mapping of the electrical double layer changes by surface plasmon resonance imaging," RSC Adv. 8, 28266–28274 (2018).